Current Noise Spectral Density and Excess Noise of a Silicon Low-Gain Avalanche Diode (LGAD)

Giuseppe Bertuccio, *Member, IEEE*, Iurii A. Eremeev, *Graduate Student Member, IEEE*, Filippo Mele, *Member, IEEE*, Jacopo Quercia, *Member, IEEE*, Wei Chen, and Gabriele Giacomini

***Abstract*— The current noise power spectral density (NPSD) of a silicon low-gain avalanche diode (LGAD) has been measured at room temperature under different bias conditions. The device has been biased in its whole operating range up to close the junction breakdown with dark currents between 100 pA and 3 nA. The NPSDs have been measured in a bandwidth from 10 Hz up to a maximum frequency ranging from 10 kHz up to 3 MHz, depending on the noise level. The NPSDs have been found white in all the operative conditions with no evidence of a $1/f$ component. An empirical law is proposed to describe the NPSD with high accuracy over four orders of magnitude from 10^{-28} to 10^{-24} A^2/Hz. The excess noise factor ζ has been experimentally determined from the NPSD and accurate measurements of the multiplication gain M. A good agreement with McIntyre's theory has been found only at higher gain values, but for $M < 30$, the excess noise has been found to be accurately predicted by the M^n law with $n = 0.632 \pm 0.014$. An extremely low value of $\zeta = 1.06 \pm 0.01$ has been measured at $M = 5$, opening perspectives to the development of ultralow-noise radiation and particle detecting systems for both timing and spectroscopy applications.**

***Index Terms*— Electrical characterization, excess noise factor, gain, low-gain avalanche diode (LGAD), noise power spectral density (NPSD), semiconductor radiation detectors.**

I. Introduction

DURING the past decades, significant research activity has been devoted to the study and development of new semiconductor particle and radiation detectors to be used in large apparatuses for high-energy physics (HEP) experiments such as the Large Hadron Collider at CERN [1]. In these experiments, one of the main challenges is to obtain the highest resolution in energy, position, and time of interaction in order to precisely reconstruct the particle tracks close to the vertex of the collisions. In order to reach the required time resolution of the order of a few tens of picoseconds, the thicknesses of silicon detectors should be limited to tens of micrometers to speed up the collection of the electron–hole (e–h) pairs generated by the ionizing particles. However, since minimum ionizing particles (MIPs) generate only about 60–80 e–h pairs per 1 μm in silicon [2], thin detectors suffer from low amplitude signals, with consequent low signal-to-noise ratio in the processing with low-power and wide-bandwidth front-end electronics. To overcome this problem, the use of silicon avalanche diodes with thin drift region (few tens of micrometers) biased in the pre-breakdown region, where they exhibit a moderate electric charge multiplication, has been proposed [3], [4], [5]. These devices are now commonly known as low-gain avalanche diodes (or detectors) (LGADs) and have been successfully manufactured and tested [6], [7], [8], [9], [10]. The electronic noise associated with the dark current of an LGAD can play a significant role in the final device and system performance, but no experimental noise power spectral densities (NPSD) of LGAD's current are available, yet. In this article, we present our work aimed to measure and analyze the NPSD and the excess noise of an LGAD.

Manuscript received 6 June 2024; revised 31 July 2024; accepted 5 August 2024. This work was supported in part by Italian Ministry for University and Research (MUR); and in part by European Union (EU) through the Project FSE REACT-EU, PON Ricerca e Innovazione 2014–2020, under Grant DM 1062/2021. The review of this article was arranged by Editor K. Stefanov. *(Corresponding author: Giuseppe Bertuccio.)*

Giuseppe Bertuccio, Iurii A. Eremeev, Filippo Mele, and Jacopo Quercia are with the Dipartimento di Elettronica, Informazione e Bioingegneria, Politecnico di Milano, 22100 Como, Italy.

Wei Chen and Gabriele Giacomini are with Instrumentation Division, Brookhaven National Laboratories, New York, NY 11973 USA.

Color versions of one or more figures in this article are available at https://doi.org/10.1109/TED.2024.3440961.

Digital Object Identifier 10.1109/TED.2024.3440961

II. Device Structure and Principle of Operation

A. Structure

Fig. 1(a) shows a schematic cross section of the LGAD designed and fabricated at the Brookhaven National Laboratory and used for this study. A low doped ($\simeq 10^{12}$ cm^{-3}) p-type 20-μm-thick epitaxial layer is realized on a low-resistivity 340-μm p^+ substrate. An ohmic contact is formed at the back. An n^+ implant on the front surface implements a rectifying junction with the underlying p layer. An external n^+ contact constitutes a guard ring for draining the current generated at the device periphery. A p-type thin layer (called

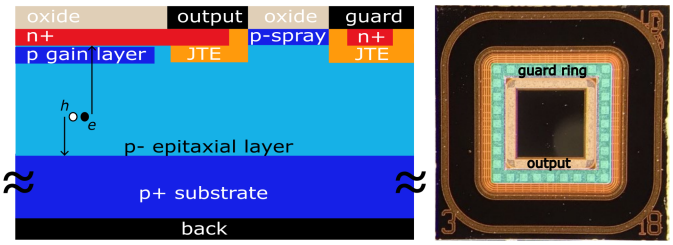

Fig. 1. (a) Schematic cross section of the LGAD structure (not to scale). (b) Micrograph of the front side of the device.

gain layer in the following) is made by ion implantation, tuned to obtain, under reverse bias condition of the junction, a peak of electric field, high enough to allow charge multiplication due to impact ionization. Junction termination extensions (JTEs) are used at the contact edge of the central and guard n^+ regions to reduce the local electric field. A p-spray layer, uniformly implanted at the beginning of the process, is used to prevent the formation of an electron accumulation layer at the oxide/silicon interface between the contacts. A photograph of the front side of the device is shown in Fig. 1(b). The n^+ output contact is square with an area of 1.3×1.3 mm^2. An identical device without the gain layer, called Diode in the following, was fabricated to be directly compared with the LGAD.

B. Principle of Operation as Radiation and Particle Detector

In operating conditions, the n^+ output electrode is connected to a transimpedance or a charge-sensitive amplifier (CSA), the guard is grounded, and the p-n junctions are reverse biased by applying a negative voltage at the p^+ back contact, to fully deplete the p^- epitaxial and the p gain layers. The detector is exposed to photons or particles at the front side, causing generation of e–h pairs in the epitaxial layer. The electrons, drifting toward the n^+ output electrode, reach the p gain layer where additional e–h pairs are generated by impact ionization. The signal multiplication gain M of the device is defined as the ratio between the charge induced at the output electrode and the charge originally generated by the photon or particle.

III. Electrical Characterization

A. I–V Characterization

The I–V characteristics of the LGAD and the Diode have been measured by applying a reverse bias voltage at the p^+ back contact while measuring the dc current simultaneously at the output and guard electrodes using two Keithley 6430 electrometers with a total resolution better than 10 fA in the picoampere range. Fig. 2 shows the I–V characteristics measured with the devices placed in a climatic chamber at a temperature of $+30$ °C $\pm$ 0.5 °C. The Diode shows a gradual increase of its reverse current until about 20 V and an almost constant reverse current between 23 and 30 pA for voltages from 20 to 120 V. The LGAD current is identical to the Diode one up to 3 V, where it starts to increase rapidly up to 100 pA at 21 V. From 21 to 113 V, the LGAD current gradually

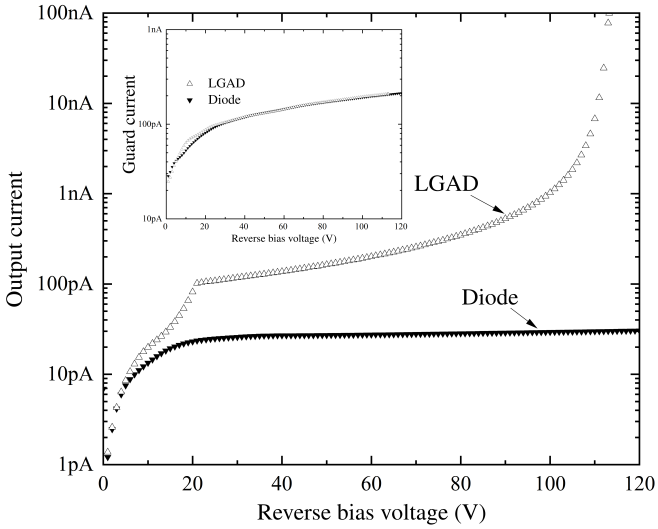

Fig. 2. I–V characteristics of the LGAD and Diode measured at $+30$ °C. In the inset, their respective guard currents are shown.

increases up to 100 nA. Avalanche breakdown occurs above 113 V. The higher LGAD current with respect to the Diode arises from the additional e–h pairs generated in the gain layer by impact ionization. It can be observed that the currents at the guard electrodes of the LGAD and the Diode are identical (Fig. 2, inset).

B. CV Characterization

The capacitance at the output electrode of the Diode and LGAD has been measured in the reverse bias voltage range from $V_{\text{bias}} = 0$ to 110 V by means of Agilent LCR meter 4284A, using a 100-mV, 10-kHz sinusoidal signal. The measured CV characteristics are shown in Fig. 3. For the Diode, the capacitance continuously decreases from 18 down to 11.2 pF as V_{bias} is increased up to 3 V; for $V_{\text{bias}} > 3$ V, the capacitance remains almost constant at about 10.5 pF because of the full depletion of the epitaxial layer. The capacitance of LGAD decreases from 617 down to 183 pF when the reverse voltage is increased from 0 up to 18 V; from 18 to 21 V, an abrupt drop down to 11.2 pF is observed. At $V_{\text{bias}} > 21$ V, the capacitance remains constant at about 10.5 pF. The high capacitance for $V_{\text{bias}} < 18$ V is caused by the thin depletion depth due to the high p-type doping of the region beneath the n^+ output contact, including the p-gain layer. When, at about 18 V, the p-gain layer is fully depleted, the p^- epitaxial layer is then depleted with a small increase of the reverse voltage due to its low doping. At voltages higher than 21 V, the whole epitaxial layer is fully depleted and the capacitance remains constant and identical to the one of the Diode, as expected, with a value in good agreement with the geometric capacitance of a 20-μm-thick planar-plate capacitor having the area of the output electrode and considering a stray capacitance of about 2 pF. The doping concentration profile of LGAD in the gain layer as derived from the CV measurements shows a peak of 4×10^{16} cm^{-3} at 600 nm from the n^+ contact.

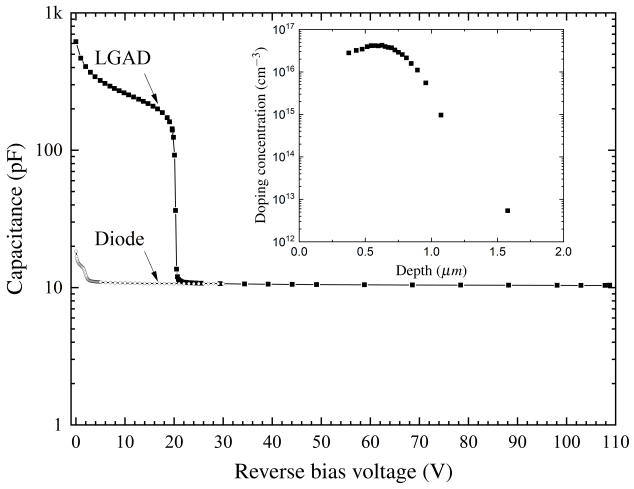

Fig. 3. LGAD capacitance is plotted with respect to the bias voltage measured at 10 kHz. In the inset, the derived doping concentration profile of the gain layer is plotted.

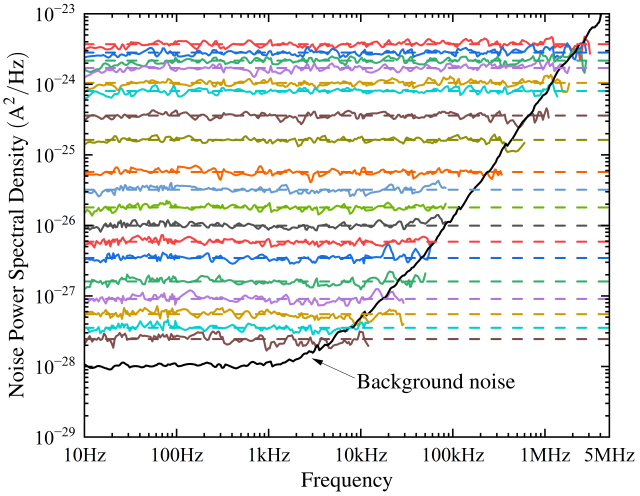

Fig. 4. Measured noise power spectral densities of the current noise generated in LGAD for the reverse bias voltages: 30, 40, 50, 60, 70, 80, 85.5, 90, 94.3, 97.7, 100, 103.8, 105.9, 107.5, 108, 108.8, 109.2, 109.6, and 110 V. Dashed lines represent the averaged values used for the noise analysis. The measured background noise of the system is shown (black curve) and determines the bandwidth of the measurements.

IV. Measuring System and Experimental NPSD

The noise power spectral densities of the LGAD have been measured using a custom-designed ultralow-noise wideband transimpedance amplifier (TIA) and an Agilent 4295A Spectrum Analyzer [11]. The measuring system has been first verified and calibrated with resistors as sources of white noise. The LGAD connected to the TIA has been placed in a climatic chamber to set a constant temperature of $+30$ °C constantly monitored with fluctuations within ± 0.5 °C. The LGAD has been reverse biased applying a negative voltage V_{bias} from -30 up to -110 V at p^+ back contact. At any bias point, the TIA dc output voltage has been first measured to exactly determine the LGAD dc current, thanks to the precise knowledge of the TIA feedback resistance R_F. The measured NPSDs are shown in Fig. 4; at each bias voltage, the bandwidth is determined by the background noise of the measuring system (shown), which limits the maximum frequency from 10 kHz to 3 MHz with the increasing of the noise level. The system background noise has been quadratically subtracted from any NPSD measurement. It can be observed that at all bias voltages, the measured NPSDs show only a white noise component with no evidence of a measurable $1/f$ component, and a variation of more than four orders of magnitude of the NPSD has been measured in the explored bias range. The dashed lines in Fig. 4 are the mean values of the measured white noises, which are determined with relative errors between $\pm 0.5\%$ and $\pm 1\%$ due to the high resolution of the measuring system.

V. Analysis and Modeling

A. Current NPSD Versus Reverse Current

The experimental power spectral density of the current white noise of the LGAD as a function of its dc reverse current I_{LGAD} is shown in Fig. 5. Over almost four orders of magnitude, as represented by the red solid line obtained with a least-squares fit to the experimental data, the average NPSD of the LGAD current $S_{I\,(\text{exp})}$ is found to be well described by the equation

$$S_{I\,(\text{exp})} = \delta \left(\frac{I_{\text{LGAD}}}{I_0} \right)^{\text{n}} \tag{1}$$

with extracted fitting parameters δ and n, being $\delta = 2qI_0 = (1.86 \pm 0.06) \times 10^{-29}$ A^2/Hz (where q is the elementary charge) and $\text{n} = 2.813 \pm 0.020$. $I_0 = \delta/2q = 58.0 \pm 1.9$ pA is a normalization constant current, introduced for dimensional consistency, which can be interpreted as the LGAD current for which the model predicts a pure shot noise $2qI_0$ (graphically given by crossing between the red solid line and the black dashed line in Fig. 5).[1] Although (1) fully describes the device's noise, it is interesting and important to analyze the dependence of the NPSD given by (1) from the multiplication gain M of the device, as it will be discussed in the next sections.

B. Models of the NPSD of Avalanche Diodes

In LGADs, as in all avalanche diodes operating in the pre-avalanche mode, the current $I_{\text{LGAD}} = I_{\text{in}}M$ is due to a primary current I_{in}, entering the gain layer, multiplied by the multiplication gain M and, in the ideal case of a deterministic gain, the NPSD would be $(2qI_{\text{in}})M^2 = (2qI_{\text{LGAD}})M$. In the real case, the NPSD is expected to be described by the theoretical equation

$$S_{I\,(\text{theory})} = 2qI_{\text{in}}M^2\zeta \tag{2}$$

in which ζ, called "excess noise factor," is higher than unity due to the additional stochastic fluctuation introduced by the ionization process, which determines the multiplication gain M [12], [13], [14].

[1] Evidently, the expression in (1) can only be valid for $I_{\text{LGAD}} \geq I_0$ and has been experimentally verified for values of $I_{\text{LGAD}} \geq 117$ pA $\simeq 2I_0$.

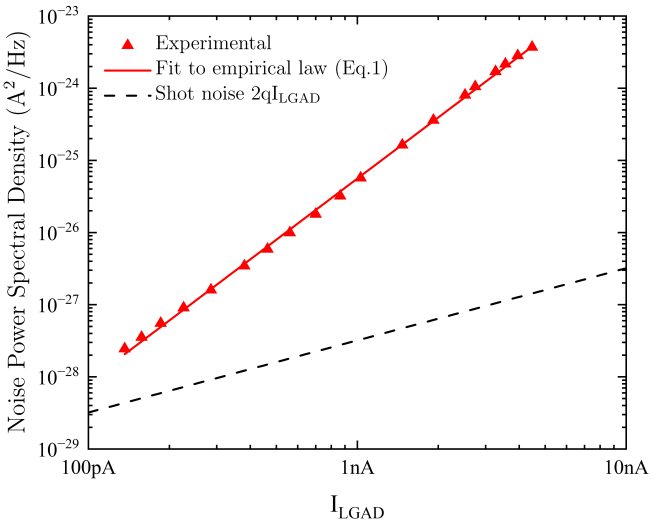

Fig. 5. NPSD of LGAD current as a function of its dc current I_{LGAD}. The experimental points are fit to the empirical law (1). In the dashed line, the shot noise of a current equal to I_{LGAD} is shown.

1) McIntyre Model: McIntyre [12] proposed a model for the noise of avalanche diode, which was experimentally verified and became a fundamental reference in many subsequent works [15]. The model, in case the carriers injected into the gain layer are electrons, predicts the NPSD as

$$S_I = (2q\,I_{\text{in}})M^2\left\{M\left[1-(1-k)\left(\frac{M-1}{M}\right)^2\right]\right\} \tag{3}$$

in which $k = \beta/\alpha$ is the ratio of the ionization coefficients of holes and electrons, respectively. The factor in curly brackets is the excess noise factor ζ, which can be rewritten as

$$\zeta = kM + (1-k)\left(2-\frac{1}{M}\right). \tag{4}$$

The model correctly predicts that in case $M = 1$ (no multiplication), $\zeta = 1$ for any value of k. For $k = 0$ (no ionization by holes), it results $\zeta = 2 - (1/M)$ so that ζ approaches $\zeta = 2$ at relatively low multiplication gain. For $k = 1$ (equal ionization coefficient for electrons and holes), the excess noise factor equals M. For $k \neq 0$ and relatively high values of M, the model predicts a linear dependence of ζ on M with a slope equal to k.

2) Empirical Model for Excess Noise: Equating the empirical (1) with the theoretical equation (2), the excess noise factor can be derived as a function of the multiplication gain, obtaining[2]

$$\zeta = \left(\frac{I_{\text{in}}}{I_0}\right)^{n-1} M^{n-2}. \tag{5}$$

Since $n = 2.813 \pm 0.02$ from the fit of the experimental data, it results that ζ is proportional to $M^{(0.813\pm0.02)}$, which is a dependence not predicted by the McIntyre model.

C. Consideration on the Excess Noise Factor

The excess noise factor ζ is an important figure of merit for photodiodes and radiation detectors operating in the pre-avalanche mode. In fact, as experimentally observed and theoretically predicted by (4) and (5), ζ increases with M, and since the device's output signal and the dark current are both proportional to M as well, the determination of ζ as function of M allows to predict the intrinsic signal-to-noise ratio of the device under different bias conditions.

However, from the NPSD experimental data, only the product $M \times \zeta = S_{I(\text{exp})}/2q\,I_{\text{LGAD}}$ can be precisely obtained so that the accuracy in the determination of ζ directly depends from the accuracy of the measurements of the multiplication gain M.

D. Determination of the Multiplication Gain

1) Signal and Dark Current Multiplication Gains: The experimental determination of the multiplication gain M is generally done by generating e–h pairs outside the multiplication region by focusing a low-intensity light or by means of ionizing radiation or particles. This procedure can be critical because it has been observed that the gain of avalanche photodiodes (APDs) depends on the wavelength of the incident light so that different values of M can be measured in the same bias condition [16]. The same occurs in LGADs, whose gain has been found to be dependent, in general, on the type of radiation (X-ray, alpha, electrons) and on the energy of the radiation quanta or particle [17]. The explanation of this phenomenon is that the multiplication process is affected by the quantity, position, and spatial distribution of the initial charge carriers, generated in the device, and also by the influence of the density of the charge cloud on the local electric field. In general, the gain derived by these measurements can be referred to as the multiplication factor M_S related to the charge signal, and it depends on the type and energy of the radiation. Differently, for the determination of the excess noise factor ζ, it is necessary to measure the multiplication factor related to the dark current, which we can indicate as M_{DC} and it can be different from M_S because of the much lower initial charge density entering into the gain layer and of a more uniform charge injection over the full sensitive area. In fact, it can be considered that an initial dark current of 20 pA, as it can be estimated in our case (see Diode in Fig. 2), corresponds to an injected flux of 1 electron every 8 ns over the whole area of the gain layer itself; differently, a single 1-keV photon (soft X-ray) generates a highly localized cloud of about 300 electrons almost simultaneously entering into the gain layer through a very small area. It is so expected that the high concentration of charge carriers derived by the multiplication could significantly lower the local electric field, causing a gain compression, implying $M_S \leq M_{\text{DC}}$. The gain M_S could approach M_{DC} in case of a uniform and weak light illumination in the epitaxial layer, i.e., in the same volume where the electron–hole pairs responsible for the dark current are thermally generated. However, this is not possible for all devices, which can be irradiated only from the side close to the gain layer, because of a passive and thick substrate on the other side, as in our case.

2) Determination of M_S From X-Gamma Rays: In order to experimentally determine M_S, the LGAD has been irradiated with X and γ rays from a ^{241}Am source placed at 1 cm from the anode of the device. The relatively high energies

[2]Accordingly to (1), (5) is valid for $I_{\text{LGAD}} = I_{\text{in}} \cdot M \geq I_0$, as well.

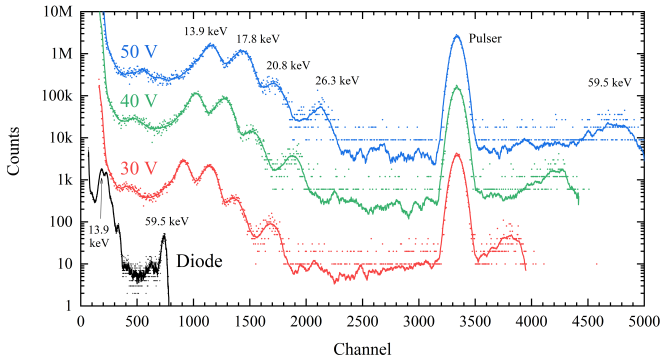

Fig. 6. Energy spectra of a ^{241}Am radioactive calibration source acquired using the LGAD biased at 30 V (red), 40 V (green), and 50 V (blue), along with the electronic pulser line; 40 and 50 V have been artificially shifted upward for better visualization. The spectrum acquired with the Diode under identical experimental conditions is shown.

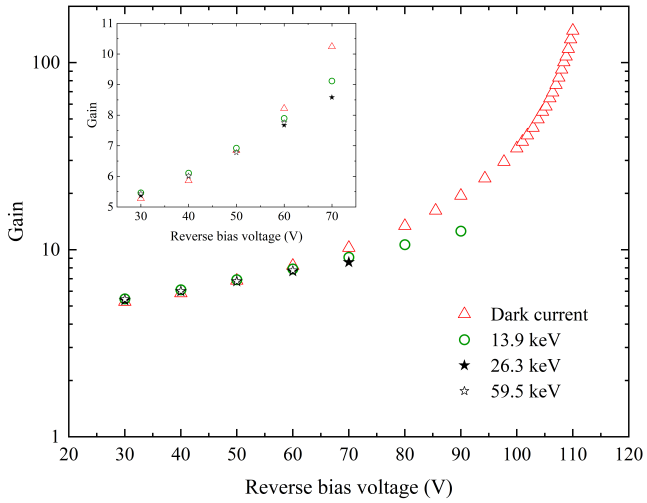

Fig. 7. LGAD gain versus bias voltage measured with ^{241}Am spectra and the gain values obtained as the ratio of dark currents.

(14–59 keV) of the ^{241}Am spectral lines allow to generate electron–hole pairs in the epitaxial region underneath the gain layer. The TIA, used as CSA, has been connected to a digital pulse processor/multichannel analyzer (Amptek PX5). A precision pulser, generating step-like voltage signals across a test capacitance connected at the CSA input, has been used to generate two artificial lines in order to calibrate and equalize the system gains when the Diode and LGAD have been connected to the CSA, respectively. The spectra have been acquired with LGAD at different bias voltages from $V_{\text{rev}} = 30$ up to 90 V and with the Diode at 40 V. Fig. 6 shows the spectrum acquired with the Diode and three of the spectra acquired with LGAD. For $V_{\text{rev}} < 20$ V (not shown), the very high LGAD capacitance causes a strong increase of electronic noise which does not allow to clearly identify the spectral lines. The positions (in ADC channels) of the peak of spectral lines at 13.9, 26.3, and 59.5 keV, compared with the corresponding lines acquired with the Diode, have been used to determine the LGAD gain M_S, which is shown in Fig. 7. The high resolution of the spectroscopic system has allowed to determine the peak of the spectral lines with a precision better than $\pm 0.5\%$ permitting to determine M_S with precision better than $\pm 1\%$. It can be observed that M_S is found almost identical at all the three photon energies up to 60 V. At 70 V, a small gain compression can be observed with a slight decrease of M_S at increasing energies (see Fig. 7, inset), and at 80 and 90 V, the increase of the total electronic noise has allowed to determine the gain with the 13.9-keV line only.

3) Determination of M_{DC} From the I–V Characteristics: In general, the value of the multiplication gain of the dark current $M_{\text{DC}} = I_{\text{LGAD}}/I_{\text{in}}$ can be determined only if the primary dark current I_{in} can be known as a function of the bias voltage. An estimate of I_{in} can be done by comparing the I–V characteristics of the LGAD and the Diode (see Fig. 2) where it can be noted that the currents at the n^+ guard electrodes of the two devices are practically identical. This equality implies that the generation currents arising from the epitaxial volume underneath the guard electrodes of the two devices are the same, which means that the density of the generation centers and the effective carrier lifetime are identical for both these LGAD and Diode samples. If this condition would have been valid also for the volume underneath the LGAD and Diode output n^+ electrodes, it would have meant that $I_{\text{in}} = I_{\text{Diode}}$ and the multiplication gain would be simply given by the ratio $M_{\text{DC}} = I_{\text{LGAD}}/I_{\text{Diode}}$, which is shown in Fig. 7. It can be observed that M_{DC} and M_S are found equal up to gains $M_S = 7$ and $V_{\text{Bias}} = 60$ V, while for higher voltages, it is observed that $M_S \leq M_{\text{DC}}$ due to the compression of the signal gain arising from the increase of the charge density in the case of the high number of electrons generated by the X–γ photons. The experimental values show that $M_{\text{DC}} = M_S$ in the bias ranges from 30 to 60 V and this condition allows to consider $I_{\text{LGAD}}/I_{\text{Diode}}$ as the gain M_{DC} to be used for the determination of ζ in the whole LGAD bias condition.

E. Excess Noise Determination

1) Full Gain Range: The excess noise factors ζ derived from the experimental values of the LGAD noise and determined as a function of M_{DC} are shown in Fig. 8. Considering the high resolution in the measurement of both the LGAD noise and gain, the errors of all the ζ data are better than $\pm 2\%$. The experimental data have been fit to the McIntyre theoretical model [see (4)—dashed lines] with k as a fitting parameter, finding $k = 0.12$. It can be seen that the McIntyre model is in excellent agreement with the experimental data for $M \geq 70$ but overestimates ζ at lower gains with error of 40% at $M = 20$ and up to 120% at $M = 5$. The fact that McIntyre's model well predicts ζ only at high gains can be justified considering that the model is based on the assumption that each carrier injected into the gain layer initiates a relatively large number of ionization events [12], which is the case of high multiplication gain, indeed. The data have been fit to the empirical model [see (5)—solid lines], as well, using the parameters n and δ derived from the dependence of NPSD on LGAD current from Fig. 5. The empirical model is in excellent agreement with the experimental data up to $M = 70$ and slightly underestimates ζ at higher gains, with errors still lower than 9%.

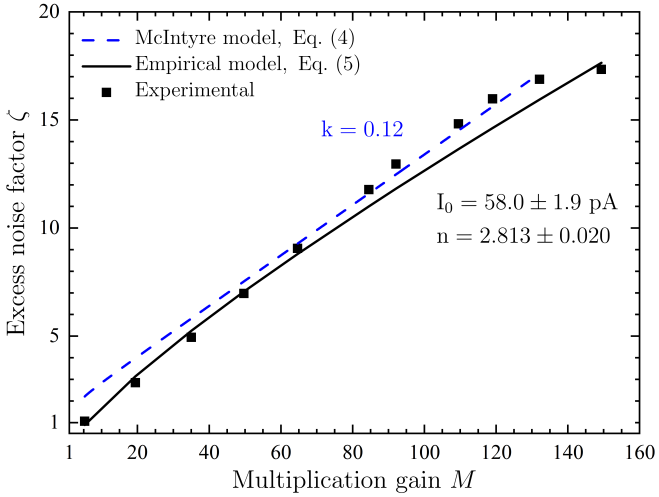

Fig. 8. Excess noise factor of LGAD extracted from noise measurements as a function of dark current gain according to Fig. 7. The empirical model with $M^{0.813}$ is shown as a solid line (5). The dashed line represents the fit to McIntyre model (4).

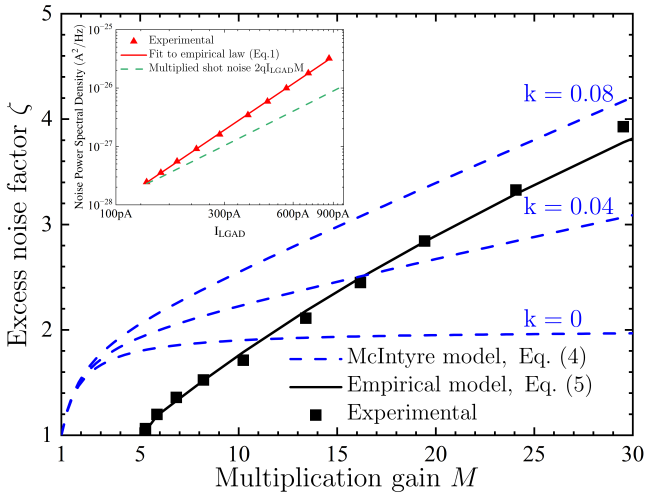

Fig. 9. Excess noise factor of LGAD extracted from noise measurements as a function of multiplication gain in the low-gain region. The empirical model (5) is shown as a solid line. The McIntyre model (4) is shown as a dashed line. The graph in the inset shows the NPSD experimental data.

2) Low-Gain Range: The low-gain range ($M < 30$) is of particular interest for applications of LGAD devices because gains of a few units or tens are sufficient to achieve adequate signal amplitudes for further processing, without the eventual degradation of the signal-to-noise ratio due to the strong increase of the excess noise at higher gains. Considering the NPSD measured at relatively low reverse bias voltages, we can obtain a more accurate fit of the NPSD versus I_{LGAD} for this specific region of interest. Fig. 9 shows the complete set of data acquired in the low-gain range, along with fits of the excess noise factor to the empirical model (solid lines). In this low-gain region, it is more evident that the McIntyre model (dashed lines) does not correctly describe the excess noise behavior, while the empirical model with $n = 2.632 \pm 0.014$ and $\delta = (1.54 \pm 0.03) \times 10^{-29}$ A^2/Hz ($I_0 = 48.10 \pm 0.87$ pA) shows an excellent agreement with the experimental data in the whole considered low-gain range. It is worthwhile to note that differently from the McIntyre model (4), which always predicts $\zeta = 1$ for $M = 1$, the empirical model (5) can predict $\zeta = 1$ also for gain $M > 1$ when $I_o > I_{\mathrm{in}}$.

F. Discussion on the Excess Noise Factor

Table I reports the lowest values of the excess noise factor measured in silicon avalanche photodiodes. It can be observed that most of the values are in the range $1.9 \leq \zeta \leq 2.5$ for gain $3 \leq M \leq 18$. This is what can be expected also on the basis of the classical McIntyre's theory, which predicts a rapid growth of the excess noise factor above unity in the $1 < M < 5$ range for any k value (see Fig. 9). Our measurements of the NPSD of the LGAD at low multiplication gain M have revealed interesting experimental results: between $M = 5$ and $M = 10$, the excess noise factors ζ have been measured lower than 1.71, and at the lowest value of gain $M = 5$, an exceptional $\zeta = 1.06 \pm 0.01$ has been measured. A value so close to unity indicates a quasi-deterministic charge multiplication and it has been measured also in Si CMOS APD [18] and, more recently, in the more complex staircase avalanche photodiodes [23]. A theoretical explanation for such low excess noise in an LGAD can be searched in the "dead space effect" [24] or "history-dependent" theory [25], which predicts a decrease of ζ well below the values expected from the classical theory as the multiplication layer becomes thinner, as experimentally demonstrated in GaAs APD [26] and Si CMOS APD [18].

TABLE I
MINIMUM EXCESS NOISE AND RELATED k FACTORS MEASURED IN SILICON APDS

Minimum ζ (gain)	Gain range	$k = \beta/\alpha$	Note
1.06 (5)	5 – 150	0.12 ($M \geq 60$)	this work
1.11 (4.5)	4 – 40	0.16–0.25 ($M \geq 15$)	380–650 nm LEDs, 2008 [18]
2.2 (3)	3 – 40	0.32	400 nm LED, 2002* [19]
2 (8.2)	5 – 105	-	380, 600 nm LEDs, 2000 [20]
1.9 (16)	8 – 4400	7.2×10^{-4}	700 nm LED, 1996 [21]
2.5 (15)	13 – 520	0.037	830 nm LED, 1976 [22]
2.4 (18)	18 – 970	0.028	830 nm LED, 1972 [15]

*the values of k are obtained by the fit of the reported data

VI. CONCLUSION

In this work, the noise power spectral density (NPSD) of a silicon LGAD has been measured in a frequency bandwidth from 10 Hz up to 3 MHz with the device under different bias conditions. The NPSD has been found white and no $1/f$ component has been observed. An empirical law (1) has been found to describe the dependence of the white noise from the dark current over almost four orders of magnitude of the NPSD. The experimental determination of the multiplication gain M at different bias voltages has been obtained by comparing the LGAD with an identical device (Diode) but without the gain layer by means of: 1) their reverse currents and 2) their response to 14-, 26-, and 59-keV X–γ photons. The two methods gave exactly the same results up to gain $M = 7$. The

excess noise factor ζ as a function of the multiplication gain M has been found to be in good agreement with the McIntyre theory only for relatively high M, while for low gain $M < 30$, an excellent agreement has been found with the empirical equation directly obtained from the NPSD. An exceptionally low $\zeta = 1.06 \pm 0.01$ has been measured at $M = 5$, which opens an interesting perspective for the further developments and applications of high energy and time resolution radiation detectors with internal charge amplification.

REFERENCES

[1] T. Szumlak, "Silicon detectors for the LHC phase-II upgrade and beyond RD50 status report," *Nucl. Instrum. Methods Phys. Res. A, Accel. Spectrom. Detect. Assoc. Equip.*, vol. 958, Apr. 2020, Art. no. 162187, doi: 10.1016/j.nima.2019.05.028.

[2] S. Meroli, D. Passeri, and L. Servoli, "Energy loss measurement for charged particles in very thin silicon layers," *J. Instrum.*, vol. 6, no. 6, Jun. 2011, Art. no. P06013, doi: 10.1088/1748-0221/6/06/p06013.

[3] H.F.-W.Sadrozinski, A. Seiden, and N. Cartiglia, "Exploring charge multiplication for fast timing with silicon sensors," presented at 20th RD50 Workshop, Bari, Italy, Jun. 2012. [Online]. Available: https://indico.cern.ch/event/175330/contributions/283780

[4] G. Pellegrini et al., "Technology developments and first measurements of low gain avalanche detectors (LGAD) for high energy physics applications," *Nucl. Instrum. Methods Phys. Res. A, Accel. Spectrom. Detect. Assoc. Equip.*, vol. 765, pp. 12–16, Nov. 2014, doi: 10.1016/j.nima.2014.06.008.

[5] G.-F. D. Betta et al., "Design and TCAD simulation of double-sided pixelated low gain avalanche detectors," *Nucl. Instrum. Methods Phys. Res. A, Accel. Spectrom. Detect. Assoc. Equip.*, vol. 796, pp. 154–157, Oct. 2015, doi: 10.1016/j.nima.2015.03.039.

[6] N. Cartiglia et al., "The 4D pixel challenge," in *Proc. 8th Int. Workshop Semicond. Pix. Det. Part. Imag. (PIXEL)*, Sestri Levante, Italy, 2016, Art. no. C12016, doi: 10.1088/1748-0221/11/12/C12016.

[7] S. Wada et al., "Evaluation of characteristics of Hamamatsu low-gain avalanche detectors," *Nucl. Instrum. Methods Phys. Res. A, Accel. Spectrom. Detect. Assoc. Equip.*, vol. 924, pp. 380–386, Apr. 2019, doi: 10.1016/j.nima.2018.09.143.

[8] G. Paternoster et al., "Novel strategies for fine-segmented low gain avalanche diodes," *Nucl. Instrum. Methods Phys. Res. A, Accel. Spectrom. Detect. Assoc. Equip.*, vol. 987, Jan. 2021, Art. no. 164840, doi: 10.1016/j.nima.2020.164840.

[9] N. Cartiglia et al., "4D tracking: Present status and perspectives," *Nucl. Instrum. Methods Phys. Res. A, Accel. Spectrom. Detect. Assoc. Equip.*, vol. 1040, Oct. 2022, Art. no. 167228, doi: 10.1016/j.nima.2022.167228.

[10] G. Giacomini, "LGAD-based silicon sensors for 4D detectors," *Sensors*, vol. 23, no. 4, p. 2132, Feb. 2023, doi: 10.3390/s23042132.

[11] I. A. Eremeev, F. Mele, J. Quercia, and G. Bertuccio, "Transimpedance amplifier for LGAD noise measurements: Design and characterization," presented at the 25th Int. Workshop Rad. Imag. Det., Lisbon, Portugal, Jul. 2024.

[12] R. J. McIntyre, "Multiplication noise in uniform avalanche diodes," *IEEE Trans. Electron Devices*, vol. ED-13, no. 1, pp. 164–168, Jan. 1966, doi: 10.1109/T-ED.1966.15651.

[13] K. M. van Vliet and L. M. Rucker, "Theory of carrier multiplication and noise in avalanche devices—Part I: One-carrier processes," *IEEE Trans. Electron Devices*, vol. ED-26, no. 5, pp. 746–751, May 1979, doi: 10.1109/T-ED.1979.19489.

[14] K. M. van Vliet, A. Friedmann, and L. M. Rucker, "Theory of carrier multiplication and noise in avalanche devices—Part II: Two-carrier processes," *IEEE Trans. Electron Devices*, vol. ED-26, no. 5, pp. 752–764, May 1979, doi: 10.1109/T-ED.1979.19490.

[15] J. Conradi, "The distribution of gains in uniformly multiplying avalanche photodiodes: Experimental," *IEEE Trans. Electron Devices*, vol. ED-19, no. 6, pp. 713–718, Jun. 1972, doi: 10.1109/t-ed.1972.17486.

[16] (Jan. 16, 2024). *Technical Note: Si APD*. Hamamatsu Photonics K.K., Hamamatsu, Japan. [Online]. Available: https://www.hamamatsu.com/content/dam/hamamatsu-photonics/sites/documents/99_SALES_LIBRARY/ssd/si-apd_kapd9007e.pdf

[17] G. Giacomini, W. Chen, G. D'Amen, E. Rossi, and A. Tricoli, "Spectroscopic performance of low-gain avalanche diodes for different types of radiation," *Nucl. Instrum. Methods Phys. Res. A, Accel. Spectrom. Detect. Assoc. Equip.*, vol. 1066, Sep. 2024, Art. no. 169605, doi: 10.1016/j.nima.2024.169605.

[18] L. Pancheri, M. Scandiuzzo, D. Stoppa, and G.-F. D. Betta, "Low-noise avalanche photodiode in standard 0.35-μm CMOS technology," *IEEE Trans. Electron Devices*, vol. 55, no. 1, pp. 457–461, Jan. 2008, doi: 10.1109/TED.2007.910570.

[19] A. Rochas, A. R. Pauchard, P.-A. Besse, D. Pantic, Z. Prijic, and R. S. Popovic, "Low-noise silicon avalanche photodiodes fabricated in conventional CMOS technologies," *IEEE Trans. Electron Devices*, vol. 49, no. 3, pp. 387–394, Mar. 2002, doi: 10.1109/16.987107.

[20] A. R. Pauchard, P.-A. Besse, and R. S. Popovic, "Dead space effect on the wavelength dependence of gain and noise in avalanche photodiodes," *IEEE Trans. Electron Devices*, vol. 47, no. 9, pp. 1685–1693, Sep. 2000, doi: 10.1109/16.861578.

[21] R. H. Redus and R. Farrell, "Gain and noise in very high-gain avalanche photodiodes: Theory and experiment," *Proc. SPIE*, vol. 2859, pp. 288–297, Jul. 1996, doi: 10.1117/12.245118.

[22] T. Kaneda, H. Matsumoto, and T. Yamaoka, "A model for reach-through avalanche photodiodes (RAPD's)," *J. Appl. Phys.*, vol. 47, no. 7, pp. 3135–3139, Jul. 1976, doi: 10.1063/1.323107.

[23] S. D. March, A. H. Jones, J. C. Campbell, and S. R. Bank, "Multistep staircase avalanche photodiodes with extremely low noise and deterministic amplification," *Nature Photon.*, vol. 15, no. 6, pp. 468–474, May 2021, doi: 10.1038/s41566-021-00814-x.

[24] J. S. Marsland, R. C. Woods, and C. A. Brownhill, "Lucky drift estimation of excess noise factor for conventional avalanche photodiodes including the dead space effect," *IEEE Trans. Electron Devices*, vol. 39, no. 5, pp. 1129–1135, May 1992, doi: 10.1109/16.129093.

[25] P. Yuan et al., "A new look at impact ionization—Part II: Gain and noise in short avalanche photodiodes," *IEEE Trans. Electron Devices*, vol. 46, no. 8, pp. 1632–1639, Aug. 1999, doi: 10.1109/16.777151.

[26] C. Hu, K. A. Anselm, B. G. Streetman, and J. C. Campbell, "Noise characteristics of thin multiplication region GaAs avalanche photodiodes," *Appl. Phys. Lett.*, vol. 69, no. 24, pp. 3734–3736, Dec. 1996, doi: 10.1063/1.117205.

Open Access funding provided by 'Politecnico di Milano' within the CRUI CARE Agreement